IMA Journal of Applied Mathematics (2008) Page 1 of 20
doi: 10.1093/imamat/dri

Micro/nano particle melting with spherical symmetry and surface tension

Scott W. McCue[1], Bisheng Wu[2] & James M. Hill[2]

[1]*School of Mathematical Sciences, Queensland University of Technology, GPO Box 2434, Brisbane QLD 4001, Australia*

[2]*Nanomechanics Group, School of Mathematics and Applied Statistics, University of Wollongong, Wollongong NSW 2522, Australia*

The process of melting a small spherical particle is treated by setting up a two-phase Stefan problem. Surface tension is included through the Gibbs-Thomson condition, the effect of which is to decrease the melting temperature as the particle radius decreases. Analytical results are derived via a small-time expansion and also through large Stefan number asymptotics. Numerical solutions are computed with a front-fixing scheme, and these results suggest that the model exhibits finite-time blow-up, in the sense that both the interface speed and the temperature gradient in the solid phase (at the interface) will become unbounded at some time before complete melting. The near blow-up behaviour appears to be similar to that encountered in the ill-posed problem of melting a superheated solid (without surface tension), and may help explain the onset of abrupt melting observed in some experiments with nanoscaled particles.

Keywords: Two-phase Stefan problem, size-dependent melting, surface tension, finite-time blow-up, superheating

1. Introduction

It is well known that surface tension acts to decrease the melting temperature of a solid particle as the radius of the particle decreases (Buffat & Borel 1976). Indeed, for very small particles this effect is nontrivial, with some metals displaying a significant reduction in melting temperature at the nanoscale (see Zhang et al. 2000, Dippel et al. 2001, Olson et al. 2005, for example, and the references therein). We consider here this phenomenon by treating a two-phase Stefan problem in a spherical domain, including the effects of surface tension modelled through the Gibbs-Thomson rule (Langer 1950).

Classical Stefan problems have received a great deal of attention in the literature. In addition to the small number of exact solutions available (for example, the Neumann solution given in Carslaw & Jaeger 1959 and Crank 1984), many approximate, semi-analytical or numerical methods have been developed. The vast majority of this research has neglected the effects of a size-dependent melting temperature, partly because most melting applications are on the macroscale, where these effects are negligible, but also because of the added mathematical difficulty that arises when the Gibbs-Thomson condition is applied at the solid-melt interface. Examples of this difficulty are that the Baiocchi transform does not apply, meaning that primitive variables must be used, and that one cannot employ the elegant enthalpy method to solve the governing equations numerically.

For the important case of melting a spherical particle, much of the existing research is

devoted to the idealised one-phase problem that arises by assuming the solid region is initially at the melting temperature. By ignoring the effects of surface tension on the solid-melt interface, this problem has been studied using a variety of analytical approaches. Of particular relevance to the present study, large Stefan number and/or near-complete-melting asymptotic analyses are given in Riley et al. (1974), Stewartson & Waechter (1976), Soward (1980) and Herrero & Velázquez (1997), and a small-time perturbation expansion is given in Davis & Hill (1982). These approaches have been extended and applied to the full two-phase version of the problem, in which the solid region may take any initial temperature, by Kucera & Hill (1986) and McCue et al. (2008).

There is a large number of numerical studies devoted to one- and two-phase Stefan problems without surface tension. For example, the commonly used enthalpy scheme (see Meyer 1973, Voller & Cross 1981, for instance) leads to reasonable results for the radially symmetric problem (Dewynne 1985). Other numerical methods are detailed in Crank (1984), including a front-fixing method, the variable time or grid step, the finite element method, the isotherm migration method, or a combination of these.

Some of the above studies have been extended to include the effects of surface tension. For example, the one-phase near-complete-melting asymptotic analysis and the small-time perturbation approach has been applied by Herraiz et al. (2001) and Wu et al. (2002), respectively, although the form of the Stefan condition used by these authors in the one-phase limit does not conserve heat on the solid-melt interface (see Evans & King 2000, King & Evans 2005 and Wu et al. 2008 for a relevant discussion). Wu et al. (2008) applied similar methods to the problem with a different boundary condition, and also presented a large Stefan number expansion.

The goal of current study is to present analytical and numerical results for the full two-phase Stefan problem of melting a spherical particle, including the effects of surface tension through a Gibbs-Thomson condition applied on the solid-melt interface. We note that the motivation for including surface tension (or kinetic undercooling, for example) in some other studies (including Dewynne et al. 1989) has been to regularise the ill-posed problem of freezing a supercooled liquid, with applications to crystal formation, for example (Gupta 2003). In that context the unregularised model may predict an unphysical singularity, such as the birth of a cusp with infinite radius of curvature (for example, see Howison et al. 1985, Velázquez 1997 and Herrero et al. 2000), and/or a solid-melt interface whose speed becomes unbounded at some finite time (see Herrero & Velázquez 1996, for instance). It may be that the inclusion of surface tension (or some other regularisation, such as kinetic undercooling) smooths these singularities, so that the solution can be continued for later times. In contrast, the present melting problem with zero surface tension is already well-posed, and here the motivation, in part, comes from understanding size-dependent thermal effects on the nanoscale, with the goal of explaining some peculiar experimental observations such as abrupt melting of nanoparticles. Remarkably, the model predicts that very small particles undergo some form of *self-superheating* when melted, and it turns out that our problem develops similar characteristics to that of the ill-posed melting problem of a superheated solid. For background on this problem, the reader is referred to Fasano & Primicerio (1977), Fasano et al. (1981), Fasano et al. (1990) and Herrero & Velázquez (1996), for example. We also remark that superheating of nanoscaled particles is discussed in the physics literature by Nanda et al. (2002) and Olsen et al. (2005), for example (although, in that context, the superheating may result from embedding the particles in a matrix of a different material).

The remainder of the paper is organised as follows. In Section 2 the governing equations

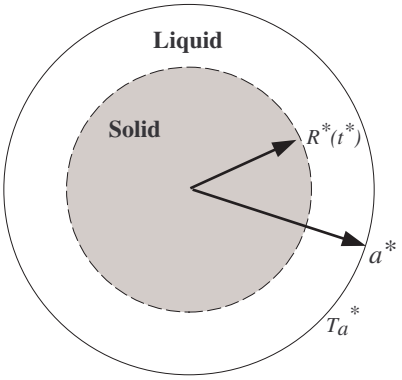

FIG. 1. Schematic of the melting particle

for the two-phase melting problem for spheres are formulated. This problem is analysed using a small-time perturbation approach in Section 3, and then a large Stefan number expansion in Section 4. Numerical results are computed using a front-fixing numerical scheme, and these are discussed in Section 5. It is shown that the analytic results derived in Sections 3 and 4 agree well with the numerical results in the appropriate regimes. Further, in the limit of slow conduction in the solid phase, numerical evidence is provided to show that the full two-phase problem does indeed reduce to the one-phase problem derived in Evans & King (2000) and Wu et al. (2008). Finally, the numerical results predict that ultimately the solid becomes (locally) superheated and, furthermore, the speed of the solid-melt interface becomes unbounded at some critical time before complete melting takes place. At this time the temperature gradient in the solid phase also becomes unbounded at the interface. This form of finite-time blow-up is discussed in Section 6, and the apparent relationship with the problem of melting a superheated solid particle noted.

2. Mathematical formulation

2.1 *Governing equations*

The geometry for the melting process under consideration is illustrated in Fig. 1. The relevant independent variables are the radial distance from the centre of the particle, r^*, and time, t^*. We suppose the particle is initially of radius a^*, and at a uniform temperature T_i^*. Then at time $t^* = 0$ the temperature on the surface $r^* = a^*$ is suddenly raised to T_a^*, and subsequently held there at that value. Provided that T_a^* is above the melting temperature, the particle will begin to melt, with a solid-melt interface $r^* = R^*(t^*)$ propagating from $r^* = a^*$ towards the centre of the particle.

The problem is to solve for the temperature distributions $T_\ell^*(r^*, t^*)$ and $T_s^*(r^*, t^*)$ in the liquid and solid phases, respectively, as well as the location of the moving boundary $r^* = R^*(t^*)$. As we are assuming heat transfers through both phases via conduction only, the governing

equations are

$$\frac{\partial T_\ell^*}{\partial t^*} = \frac{k_\ell}{\rho c_\ell}\frac{1}{r^{*2}}\frac{\partial}{\partial r^*}\left(r^{*2}\frac{\partial T_\ell^*}{\partial r^*}\right) \quad \text{in} \quad R^*(t^*) < r^* < a^*, \tag{2.1}$$

$$\frac{\partial T_s^*}{\partial t^*} = \frac{k_s}{\rho c_s}\frac{1}{r^{*2}}\frac{\partial}{\partial r^*}\left(r^{*2}\frac{\partial T_s^*}{\partial r^*}\right) \quad \text{in} \quad 0 < r^* < R^*(t^*). \tag{2.2}$$

The material parameters k_ℓ and c_ℓ are, respectively, the thermal conductivity and the specific heat capacity of the liquid phase, with the corresponding parameters for the solid phase taking the alternate subscript s. The density ρ of the material is assumed to be the same constant in each phase.

Equations (2.1)-(2.2) are supplemented with the appropriate boundary conditions, which are as follows. On the fixed boundaries we have

$$T_\ell^* = T_a^* \quad \text{on} \quad r = a^* \quad \text{and} \quad \frac{\partial T_s^*}{\partial r^*} = 0 \quad \text{on} \quad r^* = 0. \tag{2.3}$$

At the solid/liquid interface the temperature is equal to the curvature-dependent melting point $T_f^*(R^*)$:

$$T_\ell^* = T_s^* = T_f^*(R^*) \quad \text{on} \quad r^* = R^*(t^*), \tag{2.4}$$

where the form we use for $T_f^*(R^*)$ is given below. Further, the discontinuity in heat flux due to the absorbtion of latent heat L across the interface gives rise to the Stefan condition

$$k_\ell\frac{\partial T_\ell^*}{\partial r^*} - k_s\frac{\partial T_s^*}{\partial r^*} = -\rho\frac{dR^*}{dt^*}\left[(c_\ell - c_s)(T_f^* - T_m^*) + L\right] \quad \text{on} \quad r^* = R^*(t^*), \tag{2.5}$$

where T_m^* is the bulk melting point of the material (the melting temperature when the interface is flat). Finally, the initial conditions are that

$$T_s^* = T_i^*, \quad R^* = a^*, \quad \text{at} \quad t^* = 0. \tag{2.6}$$

2.2 *Gibbs-Thomsom relation*

Much research has been undertaken to relate the melting temperature to the surface (or interfacial) tension of the material. Many models, such as the homogeneous melting and growth model (Buffat & Borel 1976), the liquid shell model (Wronski 1967, Buffat & Borel 1976), and the surface-phonon instability model (Wautelet 1991) have been proposed. For a spherical nanoscaled particle, the size-dependent models based on theoretical calculations and empirical results generally take the form

$$T_f^*(R^*) = T_m^*\left(1 - \frac{\omega}{R^*}\right), \quad \omega = \frac{2\lambda}{\rho_s L}, \tag{2.7}$$

which is the Gibbs-Thomson effect (Langer 1950) mentioned in the Introduction. Here ρ_s is the mass density of the material in the solid state, and λ the interfacial tension coefficient. The homogeneous melting and growth model considers the thermodynamical equilibrium between the solid particle and the melted liquid phase. In this model, the interfacial tension coefficient, $\lambda = \lambda_{\rm HGM}$ may be expressed as

$$\lambda_{\rm HGM} = \sigma_{sv} - \sigma_{lv}(\rho_s/\rho_\ell)^{2/3}, \tag{2.8}$$

where ρ_ℓ denotes the mass density of the material in liquid state, σ_{sv} is the interfacial tension between the solid and vapor phases and σ_{lv} the interfacial tension between the liquid and vapor phases.

Table 1 contains values for these physical properties, using the metals gold, bismuth, tin and lead as examples. We see that for gold, with an atomic radius of about 0.135 nm, we have the value $\omega = 0.2396$ nm. This means that when the radius of a gold particle is $R^* = 10$ nm, containing about 200 atoms, the melting point is about 26.9 K less than the bulk melting point. This is a significant reduction.

Table 1. Physical properties for some metals

	ρ_s (kg/m^3)	ρ_l (kg/m^3)	σ_{sv} (N/m)	σ_{lv} (N/m)	L (J/kg)	T_m (K)	λ (J/m^2)	ω (nm)
Au	19.30×10^3	17.31×10^3	0.90	0.74	63718	1337.3	0.1473	0.2396
Bi	9.80×10^3	10.05×10^3	0.55	0.38	51900	544.4	0.1812	0.7126
Sn	7.27×10^3	6.99×10^3	0.66	0.55	59225	505.8	0.0957	0.4447
Pb	11.34×10^3	10.66×10^3	0.56	0.45	23020	600.6	0.0893	0.6847

2.3 *Non-dimensional equations*

We scale the problem using the dimensionless variables

$$r = \frac{r^*}{a^*}, \quad R(t) = \frac{R^*(t^*)}{a^*}, \quad t = \frac{k_\ell}{\rho c_\ell a^{*2}}\, t^*, \quad \Delta T^* = T_a^* - T_m^* \left(1 - \frac{\omega}{a^*}\right), \tag{2.9}$$

$$T_\ell(r,t) = \frac{T_\ell^*(r^*,t^*) - T_m^*(1-\omega/a^*)}{\Delta T^*}, \quad T_s(r,t) = \frac{T_s^*(r^*,t^*) - T_m^*(1-\omega/a^*)}{\Delta T^*}. \tag{2.10}$$

With these variables, the two-phase Stefan problem is

$$\frac{\partial T_\ell}{\partial t} = \frac{\partial^2 T_\ell}{\partial r^2} + \frac{2}{r}\frac{\partial T_\ell}{\partial r} \quad \text{in} \quad R(t) < r < 1, \tag{2.11}$$

$$\frac{\partial T_s}{\partial t} = \frac{\kappa}{\delta}\left(\frac{\partial^2 T_s}{\partial r^2} + \frac{2}{r}\frac{\partial T_s}{\partial r}\right) \quad \text{in} \quad 0 < r < R(t), \tag{2.12}$$

subject to the boundary conditions

$$T_\ell = 1 \quad \text{on} \quad r = 1, \tag{2.13}$$

$$T_\ell = T_s = \sigma\left(1 - \frac{1}{R}\right) \quad \text{on} \quad r = R(t), \tag{2.14}$$

$$\frac{\partial T_\ell}{\partial r} - \kappa\frac{\partial T_s}{\partial r} = -\frac{dR}{dt}\left(-\frac{\sigma(1-\delta)}{R} + \alpha\right) \quad \text{on} \quad r = R(t), \tag{2.15}$$

$$\frac{\partial T_s}{\partial r} = 0 \quad \text{on} \quad r = 0, \tag{2.16}$$

and initial conditions

$$T_s = V, \quad R = 1, \quad \text{at} \quad t = 0. \tag{2.17}$$

The five dimensionless parameters in the problem are defined by

$$\kappa = \frac{k_s}{k_\ell}, \quad \delta = \frac{c_s}{c_\ell}, \quad \sigma = \frac{\omega T_m^*}{a^* \Delta T^*}, \quad \alpha = \frac{L}{c_\ell \Delta T^*}, \quad V = \frac{T_i^* - T_m^*(1-\omega/a^*)}{\Delta T^*}.$$

These are the ratio of thermal conductivities, the ratio of specific heat capacities, the interfacial tension parameter, the Stefan number, and the dimensionless initial temperature, respectively.

3. Small time limit

Davis & Hill (1982) made use of a small time perturbation expansion in order to analyse the classical one-phase Stefan problem (without surface tension) for spherical particles initially at fusion temperature, and this technique was extended by Kucera & Hill (1986) and McCue et al. (2008) to solve the full two-phase problem. More recently, Wu et al. (2008) extended the one-phase analysis by taking into account the effects of surface tension. In this section we generalise the above studies to the full two-phase problem with surface tension.

3.1 *Summary of the details*

Our analysis follows McCue et al. (2008) closely. The idea is to look for solutions of the form

$$u \sim \frac{1}{r}\left\{A_0(X) + Y A_1(X) + O(Y^2)\right\}, \; v \sim V + \frac{1}{r}\left\{B_0(X) + Y B_1(X) + O(Y^2)\right\}, \tag{3.1}$$

as $Y \to 0^+$, where X and Y are defined by

$$X = \frac{1-r}{1-R}, \quad Y = 1 - R.$$

This change of variables transforms the inner solid phase to $1 \leqslant X < (1-R)^{-1}$ and the outer liquid phase to the fixed domain $0 \leqslant X \leqslant 1$.

After substituting (3.1) into the governing equations (2.11)-(2.12), (2.15), we find that A_0, A_1, B_0 and B_1 satisfy the coupled ordinary differential equations

$$A_0'' + \gamma X A_0' = 0, \quad A_1'' + \gamma(X A_1' - A_1) = \frac{a_1 - \gamma\alpha}{\alpha - \sigma(1-\delta)} X A_0',$$

$$\frac{\kappa}{\delta} B_0'' + \gamma X B_0' = 0, \quad \frac{\kappa}{\delta} B_1'' + \gamma(X B_1' - B_1) = \frac{a_1 - \gamma\alpha}{\alpha - \sigma(1-\delta)} X B_0',$$

where

$$\gamma = -\frac{A_0'(1) - \kappa B_0'(1)}{\alpha - \sigma(1-\delta)}, \quad a_1 = A_1'(1) - \kappa B_1'(1) + \kappa V.$$

From (2.13)-(2.14), (2.17), we have the boundary conditions

$$A_0 = 1, \quad A_1 = 0, \quad \text{on} \quad X = 0,$$

$$A_0 = 0, \quad A_1 = -\sigma, \quad B_0 = -V, \quad B_1 = V - \sigma \quad \text{on} \quad X = 1,$$

$$B_0 = o(1), \quad B_1 = o(X), \quad \text{as} \quad X \to \infty.$$

The leading order solutions are

$$A_0 = 1 - \frac{\operatorname{erf}\left(\sqrt{\frac{\gamma}{2}}\,X\right)}{\operatorname{erf}\sqrt{\frac{\gamma}{2}}}, \quad B_0 = -V\,\frac{\operatorname{erfc}\left(\sqrt{\frac{\delta\gamma}{2\kappa}}\,X\right)}{\operatorname{erfc}\sqrt{\frac{\delta\gamma}{2\kappa}}}, \tag{3.2}$$

where γ is the solution to

$$\gamma(\alpha - \sigma(1-\delta)) = \frac{1}{L_\ell}e^{-\gamma/2} + \frac{\kappa V}{L_s}e^{-\delta\gamma/2\kappa}, \tag{3.3}$$

with L_ℓ and L_s defined by

$$L_\ell = \sqrt{\frac{\pi}{2\gamma}}\operatorname{erf}\sqrt{\frac{\gamma}{2}}, \quad L_s = \sqrt{\frac{\kappa\pi}{2\delta\gamma}}\operatorname{erfc}\sqrt{\frac{\delta\gamma}{2\kappa}}. \tag{3.4}$$

The solution (3.2) together with the transcendental equation (3.3) is almost identical to the well known Neumann solution (Carslaw & Jaeger, page 285), the only difference being that in the Neumann solution (which is for zero surface tension), the term $\alpha - \sigma(1-\delta)$ in (3.3) is replaced by α. The correction terms are

$$A_1 = -\sigma X + c_1\,X\left(1 - e^{\gamma(1-X^2)/2}\right),$$

$$B_1 = c_2\left[e^{-\delta\gamma X^2/2\kappa} - \sqrt{\frac{\delta\gamma\pi}{2\kappa}}\,X\operatorname{erfc}\left(\sqrt{\frac{\delta\gamma}{2\kappa}}X\right)\right] + c_3\,Xe^{-\delta\gamma X^2/2\kappa}, \tag{3.5}$$

where

$$c_1 = \frac{1}{3\gamma}\left(\frac{\gamma\alpha - a_1}{\alpha - \sigma(1-\delta)}\right)\frac{1}{L_\ell}e^{-\gamma/2}, \quad c_3 = \frac{V}{3\gamma L_s}\left(\frac{\gamma\alpha - a_1}{\alpha - \sigma(1-\delta)}\right), \tag{3.6}$$

$$c_2 = \frac{\kappa}{\delta\gamma L_s}\left\{\sigma - V\left[1 - \frac{1}{3\gamma}\left(\frac{\gamma\alpha - a_1}{\alpha - \sigma(1-\delta)}\right)\frac{1}{L_s}e^{-\delta\gamma/2\kappa}\right]\right\}\left[1 - \frac{\kappa}{\delta\gamma L_s}e^{-\delta\gamma/2\kappa}\right]^{-1},$$

$$\frac{\gamma\alpha - a_1}{\alpha - \sigma(1-\delta)} = \frac{3\left(\gamma\alpha + \sigma - \kappa V + \kappa(V-\sigma)\left[1 - \frac{\kappa}{\delta\gamma L_s}e^{-\delta\gamma/2\kappa}\right]^{-1}\right)}{(3+\gamma)(\alpha - \sigma(1-\delta)) + \frac{V}{\gamma L_s}e^{-\delta\gamma/2\kappa}\left\{\kappa\left[1 - \frac{\kappa}{\delta\gamma L_s}e^{-\delta\gamma/2\kappa}\right]^{-1} - \kappa\gamma - \kappa + \delta\gamma\right\}}.$$

From the Stefan condition (2.15) we have the small time behaviour

$$t = \frac{1}{2\gamma}(1-R)^2 - \frac{1}{3\gamma^2}\left(\frac{\gamma\alpha - a_1}{\alpha - \sigma(1-\delta)}\right)(1-R)^3 + O((1-R)^4) \quad \text{as} \quad R \to 1^-. \tag{3.7}$$

As discussed in McCue et al. (2008), the solution described above does not satisfy the no-flux condition (2.16) at $r = 0$, and indeed by the very nature of this approach, one boundary condition must be sacrificed. However, we can easily derive an excellent approximate solution for $t \ll 1$ by changing $(3.1)_2$ to be

$$v \approx V + \frac{1}{r}\left\{B_0(X) - B_0(2Y^{-1} - X) + YB_1(X) - YB_1(2Y^{-1} - X)\right\},$$

where B_0 and B_1 are presented in (3.2) and (3.5). Given that $2Y^{-1} - X = (1+r)/(1-R)$, this alteration can be thought of as adding an image solution in the domain $-1 \leqslant r < 0$. The effect of this change is the new solution now satisfies (2.11)-(2.13) and (2.16)-(2.17) exactly, but only satisfies (2.14)-(2.15) approximately; however, the errors from (2.14)-(2.15) are exponentially small in Y as $Y \to 0^+$.

3.2 *Boundary layer near $r = 1$*

For later reference we note that for $X - 1 = O(Y)$ with $Y \ll 1$, we have

$$v \sim \frac{V}{L_s} e^{-\delta\gamma/2\kappa}(X-1) - \sigma Y + O(Y^2), \tag{3.8}$$

which describes the temperature in the solid phase in the boundary layer near $r = 1$ as $t \to 0^+$.

3.3 *Slow diffusion limit of small-time analysis*

In the limit $\kappa \to 0$, the transcendental equation (3.3) becomes

$$\gamma(\alpha - \sigma(1-\delta) - \delta V) = \frac{1}{L_\ell} e^{-\gamma/2}$$

and the constant c_1 in (3.6) becomes

$$c_1 = \frac{\gamma(\alpha + \delta\sigma - \delta V) + \sigma}{3 + \gamma}.$$

These two results agree with the small-time analysis of the one-phase problem studied in Wu et al. (2008), which is as expected.

4. Large Stefan number limit

In this section we generalise the large Stefan number analysis of McCue et al. (2008), which was for the classical two-phase problem, to allow for surface tension on the solid-melt interface. In this limit the interface moves slowly, because of the large amount of latent heat being absorbed there. For early times the surface tension has no qualitative effect on the melting process, and the details follow McCue et al. (2008) very closely. For later times, the temperature in the solid phase decays very quickly to zero for the classical case $\sigma = 0$; however, for $\sigma \neq 0$ the leading order temperature in the solid follows the variable melting temperature, and correction terms ultimately lead to local superheating. That is, after some point in time we find the temperature in the solid phase will be everywhere greater than the melting temperature (which is of course less than the bulk melting temperature).

4.1 *Time-scale $t = O(1)$*

On the first time-scale, which is $t = O(1)$, heat diffuses a distance $O(1)$ (provided $\kappa = O(1)$), but the interface only propagates a distance $O(\alpha^{-1/2})$. Thus a boundary layer develops near $r = 1$.

4.1.1 *Inner region,* $1 - r = O(\alpha^{-1/2})$ For the inner region we scale the spatial variables as $r = 1 - \alpha^{-1/2}\tilde{r}$, $R(t) = 1 - \alpha^{-1/2}\tilde{R}(t)$, and write

$$u \sim \tilde{u}_0(\tilde{r}, t) + \frac{1}{\alpha^{1/2}}\tilde{u}_1(\tilde{r}, t) + O(\alpha^{-1}), \quad v \sim \frac{1}{\alpha^{1/2}}\tilde{v}_1(\tilde{r}, t) + O(\alpha^{-1}),$$

$$\tilde{R} \sim \tilde{R}_0(t) + \frac{1}{\alpha^{1/2}}\tilde{R}_1(t) + O(\alpha^{-1}) \quad \text{as} \quad \alpha \to \infty.$$

The leading order problem for $\tilde{u}_0$, namely

$$\frac{\partial^2 \tilde{u}_0}{\partial \tilde{r}^2} = 0 \quad \text{in} \quad 0 < \tilde{r} < \tilde{R}_0, \tag{4.1}$$

$$\tilde{u}_0 = 1 \quad \text{on} \quad \tilde{r} = 0, \quad \tilde{u}_0 = 0, \quad \frac{\partial \tilde{u}_0}{\partial \tilde{r}} = -\frac{d\tilde{R}_0}{dt} \quad \text{on} \quad \tilde{r} = \tilde{R}_0, \tag{4.2}$$

has the solution

$$\tilde{u}_0 = 1 - \frac{\tilde{r}}{\tilde{R}_0}, \quad \tilde{R}_0 = \sqrt{2t}. \tag{4.3}$$

Note that solution is independent of the surface tension σ, and is thus identical to that given in McCue et al. (2008).

The next order problems are

$$\frac{\partial^2 \tilde{u}_1}{\partial \tilde{r}^2} = 2\frac{\partial \tilde{u}_0}{\partial \tilde{r}} \quad \text{in} \quad 0 < \tilde{r} < \tilde{R}_0, \quad \frac{\partial^2 \tilde{v}_1}{\partial \tilde{r}^2} = 0 \quad \text{in} \quad \tilde{r} > \tilde{R}_0, \tag{4.4}$$

with boundary conditions

$$\tilde{u}_1 = 0 \quad \text{on} \quad \tilde{r} = 0, \tag{4.5}$$

$$\tilde{u}_1 + \tilde{R}_1\frac{\partial \tilde{u}_0}{\partial \tilde{r}} = -\sigma\tilde{R}_0, \quad \tilde{v}_1 = -\sigma\tilde{R}_0, \quad \frac{\partial \tilde{u}_1}{\partial \tilde{r}} - \kappa\frac{\partial \tilde{v}_1}{\partial \tilde{r}} = -\frac{d\tilde{R}_1}{dt} \quad \text{on} \quad \tilde{r} = \tilde{R}_0, \tag{4.6}$$

$$\tilde{v}_1 \sim \tilde{a}_1(t)\tilde{r} \quad \text{as} \quad \tilde{r} \to \infty. \tag{4.7}$$

The function $\tilde{a}_1(t)$ will be determined by matching with the outer region, as described below.

In terms of $\tilde{a}_1(t)$ the solutions to (4.4)-(4.7) are

$$\tilde{u}_1 = -\frac{1}{\tilde{R}_0}\tilde{r}^2 + \left(1 - \sigma + \frac{\tilde{R}_1}{\tilde{R}_0^2}\right)\tilde{r}, \quad \tilde{v}_1 = \tilde{a}_1(\tilde{r} - \tilde{R}_0) - \sigma\tilde{R}_0,$$

with $\tilde{R}_0$ given in (4.3) and $\tilde{R}_1$ satisfying the differential equation

$$\frac{d\tilde{R}_1}{dt} + \frac{\tilde{R}_1}{\tilde{R}_0^2} = 1 + \sigma + \kappa\tilde{a}_1 \tag{4.8}$$

and initial condition $\tilde{R}_1(0) = 0$.

4.1.2 *Outer region,* $1 - r = O(1)$ The outer region is for $1 - r = O(1)$. Here we write $v = \bar{v}(r, t)$, where

$$\frac{\partial \bar{v}}{\partial t} = \frac{\kappa}{\delta}\left(\frac{\partial^2 \bar{v}}{\partial r^2} + \frac{2}{r}\frac{\partial \bar{v}}{\partial r}\right) \quad \text{in} \quad 0 < r < 1,$$

$$\bar{v} = 0 \quad \text{on} \quad r = 1, \quad \frac{\partial \bar{v}}{\partial r} = 0 \quad \text{on} \quad r = 0, \quad \bar{v} = V \quad \text{at} \quad t = 0.$$

The solution for $\bar{v}$ is

$$\bar{v} = \frac{2V}{\pi r}\sum_{n=1}^{\infty}\frac{(-1)^{n+1}}{n}\sin(n\pi r)e^{-n^2\pi^2\kappa\, t/\delta}. \tag{4.9}$$

4.1.3 *Matching between regions* By rewriting (4.9) in inner variables $(\tilde{r}, t)$ and expanding as $\alpha \to \infty$ we find

$$\tilde{v}_1 \sim 2V\tilde{r}\sum_{n=1}^{\infty} e^{-n^2\pi^2\kappa\, t/\delta} \quad \text{as} \quad \tilde{r} \to \infty.$$

Thus matching between the two regions gives

$$\tilde{a}_1 = 2V\sum_{n=1}^{\infty} e^{-n^2\pi^2\kappa\, t/\delta}, \quad \tilde{v}_1 = 2V(\tilde{r} - \tilde{R}_0)\sum_{n=1}^{\infty} e^{-n^2\pi^2\kappa\, t/\delta} - \sigma\tilde{R}_0. \tag{4.10}$$

We may now solve (4.8) for the moving boundary location, yielding

$$\tilde{R}_1 = \tfrac{2}{3}(1+\sigma)t + V\sum_{n=1}^{\infty}\left\{\frac{2e^{-n^2\pi^2\kappa\, t/\delta}}{n^2\pi^2} - \frac{\delta^{1/2}\mathrm{erf}\left(\pi n\sqrt{\kappa t/\delta}\right)}{n^3\pi^{5/2}\kappa^{1/2}t^{1/2}}\right\}.$$

As a check on the analysis, and to ensure it is consistent with that presented in Section 3, we note that

$$\sum_{n=1}^{\infty} e^{-n^2\pi^2\kappa\, t/\delta} \sim \frac{\delta^{1/2}}{2(\pi\kappa t)^{1/2}} = \sqrt{\frac{\delta}{2\pi\kappa}}\,\frac{1}{\tilde{R}_0} \quad \text{as} \quad \tilde{R}_0 \to 0.$$

Using original variables this implies that in the boundary layer we have

$$v \sim V\sqrt{\frac{2\delta}{\pi\kappa}}\left(\frac{R-r}{1-R}\right) - \sigma(1-R) \quad \text{as} \quad R \to 1^-,$$

which is seen to agree with (3.8) once it is noted from (3.3) and (3.4) that

$$\alpha \sim \gamma^{-1}, \quad \frac{1}{L_s}e^{-\delta\gamma/2\kappa} \sim \sqrt{\frac{2\delta\gamma}{\pi\kappa}} \quad \text{as} \quad \gamma \to 0.$$

A similar argument shows that the location of the interface agrees with that derived in Section 3 (see McCue et al. 2008 for details).

4.1.4 *Summary of time-scale $t = O(1)$* On the time-scale $t = O(1)$ we see that near the moving boundary the temperature in both phases has an algebraic dependence on the small parameter $\alpha^{-1/2}$. Furthermore, the two phases are coupled, although to leading order both the temperature in the solid and location of the free boundary are independent of the liquid phase. Note that the inclusion of surface tension has no qualitative effect on the solution on this time-scale.

4.2 *Time-scale $t = O(\alpha)$*

On the time-scale $t = O(\alpha)$ the solid-melt interface moves a distance $O(1)$. We rescale time as $t = \alpha\hat{t}$, where $\hat{t} = O(1)$, and look for solutions of the form

$$T_\ell = \hat{u}_0(r,R) + \frac{1}{\alpha}\hat{u}_1(r,R) + O(\alpha^{-2}), \quad T_s = \hat{v}_0(r,R) + \frac{1}{\alpha}\hat{v}_1(r,R) + \ldots + \hat{w}(r,R;\alpha), \quad (4.11)$$

$$\hat{t} = \hat{t}_0(R) + \frac{1}{\alpha}\,\hat{t}_1(R) + \ldots + \hat{\tau}(R;\alpha) \quad \text{as} \quad \alpha \to \infty. \quad (4.12)$$

The ellipses in (4.11)-(4.12) denote terms which are $O(\alpha^{-2})$ *and* independent of the initial temperature V, while the terms $\hat{w}(r,R;\alpha)$ and $\hat{\tau}(R;\alpha)$ are exponentially small in α (and will depend on V).

The problems for $\hat{u}_i$ and $\hat{v}_i$ $(i = 0, 1)$ are all elliptic (with no initial conditions); they are

$$\frac{1}{r^2}\frac{\partial}{\partial r}\left(r^2\frac{\partial \hat{u}_0}{\partial r}\right) = 0 \quad \text{on} \quad R < r < 1, \quad \frac{1}{r^2}\frac{\partial}{\partial r}\left(r^2\frac{\partial \hat{v}_0}{\partial r}\right) = 0 \quad \text{on} \quad 0 < r < R,$$

$$\hat{u}_0 = 1 \quad \text{on} \quad r = 1, \quad \hat{u}_0 = \hat{v}_0 = \sigma\left(1 - \frac{1}{R}\right) \quad \text{on} \quad r = R, \quad \frac{\partial \hat{v}_0}{\partial r} = 0 \quad \text{on} \quad r = 0,$$

$$\hat{t}_0'\left(\frac{\partial \hat{u}_0}{\partial r} - \kappa\frac{\partial \hat{v}_0}{\partial r}\right) = -1 \quad \text{on} \quad r = R,$$

$$\frac{1}{r^2}\frac{\partial}{\partial r}\left(r^2\frac{\partial \hat{u}_1}{\partial r}\right) = \frac{1}{\hat{t}_0'}\frac{\partial \hat{u}_0}{\partial R} \quad \text{on} \quad R < r < 1, \quad \frac{1}{r^2}\frac{\partial}{\partial r}\left(r^2\frac{\partial \hat{v}_1}{\partial r}\right) = \frac{1}{\hat{t}_0'}\frac{\partial \hat{v}_0}{\partial R} \quad \text{on} \quad 0 < r < R,$$

$$\hat{u}_1 = 0 \quad \text{on} \quad r = 1 \quad \hat{u}_1 = \hat{v}_1 = 0 \quad \text{on} \quad r = R, \quad \frac{\partial \hat{v}_1}{\partial r} = 0 \quad \text{on} \quad r = 0,$$

$$\hat{t}_1'\left(\frac{\partial \hat{u}_0}{\partial r} - \kappa\frac{\partial \hat{v}_0}{\partial r}\right) + \hat{t}_0'\left(\frac{\partial \hat{u}_1}{\partial r} - \kappa\frac{\partial \hat{v}_1}{\partial r}\right) = \frac{(1-\delta)\sigma}{R} \quad \text{on} \quad r = R,$$

with solutions

$$\hat{u}_0 = \frac{1}{r}\left[1-\left(\frac{1-r}{1-R}\right)\right]+\sigma\left(1-\frac{1}{r}\right), \tag{4.13}$$

$$\hat{v}_0 = \sigma\left(1-\frac{1}{R}\right), \tag{4.14}$$

$$\hat{t}_0 = -\frac{\sigma^2(1-R)}{(1-\sigma)^3}+\frac{(1-2\sigma)(1-R)^2}{2(1-\sigma)^2}-\frac{(1-R)^3}{3(1-\sigma)}-\frac{\sigma^2\ln\left[R+\sigma(1-R)\right]}{(1-\sigma)^4}, \tag{4.15}$$

$$\hat{u}_1 = -\frac{R+\sigma(1-R)}{6rR^2}\left(\frac{1-r}{1-R}\right)\left[1-\left(\frac{1-r}{1-R}\right)^2\right], \tag{4.16}$$

$$\hat{v}_1 = -\frac{\sigma\delta[R+\sigma(1-R)]}{6\kappa R^4(1-R)}(r^2-R^2), \tag{4.17}$$

$$\hat{t}_1 = \frac{1-\delta\sigma-3\sigma(1-\delta)}{3}\left\{\frac{\sigma(1-R)}{(1-\sigma)^2}+\frac{(1-R)^2}{2(1-\sigma)}+\frac{\sigma\ln\left[R+\sigma(1-R)\right]}{(1-\sigma)^3}\right\}. \tag{4.18}$$

The function $\hat{w}(r,R;\alpha)$ satisfies

$$\frac{1}{\alpha}\frac{\partial\hat{w}}{\partial\hat{t}}=\frac{\kappa}{\delta}\left(\frac{\partial^2\hat{w}}{\partial r^2}+\frac{2}{r}\frac{\partial\hat{w}}{\partial r}\right) \quad \text{in} \quad 0<r<R,$$

$$\frac{\partial\hat{w}}{\partial r}=0 \quad \text{on} \quad r=0, \quad \hat{w}=0 \quad \text{on} \quad r=R,$$

and an initial condition which comes from matching with the first time-scale. For this problem we may think of R as being a given function of $\hat{t}$. As explained in McCue et al. (2008), in the limit $\alpha\to\infty$ we may write $\hat{w}\sim e^{-\alpha g(\hat{t})}\left(\hat{w}_0(\rho)+O(\alpha^{-1})\right)$, where $\rho=r/R$ to derive an eigenvalue problem for $\hat{w}_0$. The result is that

$$\hat{w}\sim\frac{kR}{r}\sin\left(\frac{\pi r}{R}\right)\exp\left\{-\frac{\pi^2\kappa\alpha}{\delta}\int_0^{\hat{t}}\frac{d\hat{t}}{R^2}\right\} \quad \text{as} \quad \alpha\to\infty, \tag{4.19}$$

where k is a constant determined as follows. By writing out T_s (given by (4.11), (4.14)-(4.17) and (4.19)), in the variables used on the first time-scale, we find

$$T_s\sim\frac{1}{\alpha^{1/2}}\left(-\sigma\tilde{R}+k\pi(\tilde{r}-\tilde{R})e^{-\pi^2\kappa\tilde{R}^2/2\delta}\right),$$

so by matching with $\tilde{v}_1$ in (4.10) we conclude that $k=2V/\pi$. Finally, we calculate $\hat{\tau}$ via the condition

$$\frac{d\hat{\tau}}{dR}\sim-\kappa\left(\frac{\partial\hat{u}_0}{\partial r}\right)^{-2}\frac{\partial\hat{w}}{\partial r} \quad \text{on} \quad r=R,$$

which gives

$$\hat{\tau}\sim 2\kappa V\int_R^1\frac{\xi^2(1-\xi)^2}{[\xi+\sigma(1-\xi)]^2}\exp\left\{\frac{\pi^2\kappa\alpha}{\delta}\left[\frac{1-\xi}{1-\sigma}+\frac{\ln[\xi+\sigma(1-\xi)]}{(1-\sigma)^2}\right]\right\}d\xi \quad \text{as} \quad \alpha\to\infty. \tag{4.20}$$

4.2.1 *Summary of time-scale $t = O(\alpha)$* On the time-scale $t = O(\alpha)$ we see that the temperature in both phases has an algebraic dependence on the small parameter α^{-1}, although the terms involving V are are exponentially small in α. The implication is that for large Stefan numbers the melting process ultimately 'forgets' the initial condition $v = V$, and henceforth the temperature in the solid phase is driven by surface tension alone. Furthermore, given that $\hat{v}_0 + \hat{v}_1/\alpha$ is parabolic in shape with a maximum at $r = 0$, the solid becomes superheated, with the temperature everywhere greater than the melting temperature.

5. Numerical results

The problem (2.11)-(2.17) was solved numerically with a front-fixing method (Crank 1984), which involves mapping the moving boundary problem into a fixed boundary problem with a Landau-type transformation. Central finite differences were then used to approximate the spatial derivatives, and forward finite differences were employed for the temporal derivatives. Typically, we used 120 spatial grid points in the solid phase, and 80 in the liquid. The appropriate time step Δt was chosen using Von Neumann's method (Smith 1985), ensuring that the resulting scheme was stable (typically $\Delta t = O(10^{-8})$). As a test of the scheme, solutions for the classical case $\sigma = 0$ were computed using an enthalpy method, with the two different numerical approaches agreeing quite well over the full range of parameter values. Note that the enthalpy method cannot be applied to the more general problem with $\sigma \neq 0$, since the melting temperature is not constant in that case.

Typical temperature profiles are drawn in Fig. 2 for the parameter values $\alpha = 1$, $\kappa = 1$, $\delta = 1$, $V = -1$, $\sigma = 0.1$. In part (a), numerical solutions are compared with the small-time approximation derived in Section 3, and they are seen to be in excellent agreement with each other. On this time-scale the melting temperature is almost constant, and so the surface tension has no significant qualitative effect on the solutions. For later times, numerical profiles are drawn in part (b) using the same parameters. We see that as the melting temperature decreases, there is a point in time after which the solid is locally superheated, with the temperature everywhere greater than the melting temperature (which, of course, is dependent on the size of the particle). We believe that this phenomenon (which could be referred to as *self-superheating*) is followed by a form of blow-up with $\partial T_s/\partial r(R,t) \to -\infty$, $\dot{R} \to -\infty$ as $R \to R_c^+$ and $t \to t_c^-$, where $R_c > 0$ is some critical radius and $t_c < \infty$ is the corresponding time at blow-up. We discuss the point further below.

A representative solution for large Stefan numbers is presented in Fig. 3. Here the Stefan number is $\alpha = 10$, and the other parameters are the same as in Fig. 2. Included in the figure is the numerical solution, as well as the large Stefan number approximation given in Section 4. We see the asymptotic solution agrees extremely well with the numerical solution, except for late times in the liquid phase. Note the parabolic shape of the temperature in the solid phase for the profile with $R = 0.1$. Although not entirely clear on this scale, the curve is concave down, meaning the solid is superheated at that stage. Again, we predict the solution will cease to exist before complete melting takes place, however we have observed that the critical radius R_c decreases as the Stefan number increases. We expect that $R_c \to 0^+$ as $\alpha \to \infty$, since the infinite latent heat limit implies the interface will always be able to absorb the surrounding heat energy, thereby preventing blow-up. See Section 6 for a related discussion.

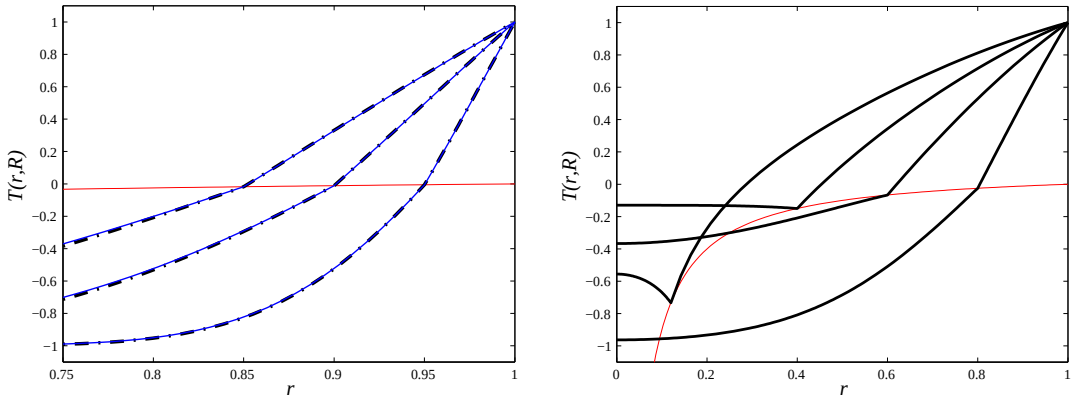

FIG. 2. Temperature profiles for $\alpha = 1$, $\kappa = 1$, $\delta = 1$, $V = -1$, $\sigma = 0.1$. In part (a), the solid curves represent the numerical solution, while the dot-dashed curves are the small-time approximations; from right to left, the profiles are for $t = 0.0033$, 0.013 and 0.028. Part (b) shows only numerical solutions; from right to left (in the liquid phase), the profiles are for $t = 0.045$, 0.124, 0.194 and 0.245. The very thin curve in both parts denotes the melting temperature.

It is of interest to compare numerical solutions of (2.11)-(2.17) for a small value of κ to the corresponding solutions of the one-phase problem derived in Wu et al. (2008) (see also Evans & King 2000) via the singular limit $\kappa \to \infty$. This is done in Fig. 4 using the same parameters as Fig. 2, except that $\kappa = 0.05$. In this figure the dot-dashed curves in the liquid phase represent numerical solutions to the one-phase problem, while dot-dashed curves in the solid phase are drawn using asymptotic results given in Evans & King (2000) and Wu et al. (2008), namely

$$\tilde{T}_s \sim V + \left[\sigma\left(1 - \frac{1}{R}\right) - V\right] \exp\left(\frac{\delta \dot{R}(R-r)}{\kappa}\right),$$

where the interface speed $\dot{R}$ is taken from the numerical solution to the one-phase problem. We see the agreement between these two approaches is excellent. Again, it is worth noting how superheating develops in the solid phase, which we expect leads to blow-up, as described above. Wu et al. (2008) suggest that in the limit $\kappa \to 0$, the blow-up will occur at the critical radius $R_c = \sigma/(\alpha + \delta(\sigma - V))$. Using the parameter values used for this figure, that would be roughly $R_c = 0.048$. The profile drawn in the figure for $R = 0.05$ appears to be very close to blow-up, which is consistent with the one-phase prediction.

In order to illustrate a solution for a small Stefan number, and also to indicate more clearly the behaviour of the melting process for late times, we present in Fig. 5 temperature profiles for $\alpha = 0.1$, $\kappa = 1$, $\delta = 1$, $V = -1$ and $\sigma = 0.05$. For these parameter values, the numerical results suggest that finite-time blow-up will occur roughly between $R = 0.12$ and 0.13. A characterising feature of the solutions with small Stefan number is that blow-up appears to occur very soon after the solid becomes superheated. We see this in part (b) of this figure, where a roughly flat profile for $R = 0.2$ evolves very quickly to one which appears to have an unbounded temperature gradient in the blow-up limit. Figure 6 illustrates the dependence of

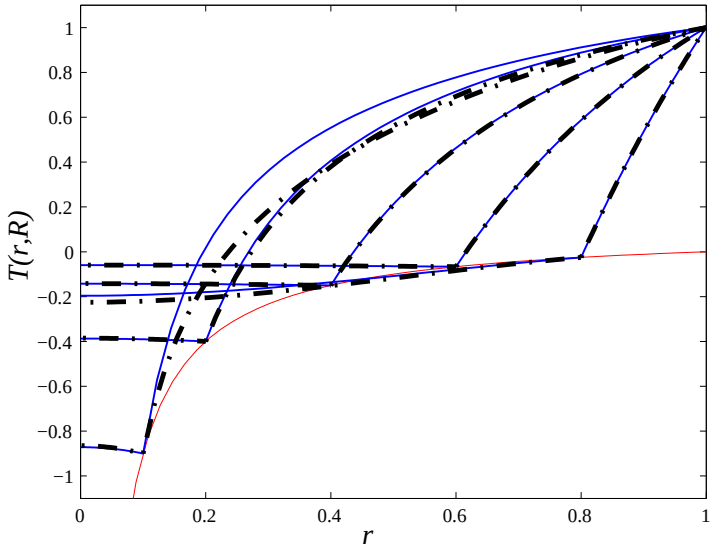

FIG. 3. Temperature profiles for $\alpha = 10$, $\kappa = 1$, $\delta = 1$, $V = -1$, $\sigma = 0.1$. The solid curves represent the numerical solution, while the dot-dashed curves come from the large Stefan number asymptotics; from right to left (in the liquid phase), the profiles are for $t = 0.197$, 0.612, 1.086, 1.452 and 1.547. The very thin curve denotes the melting temperature.

the interface speed $\dot{R}$ on the particle radius R for the same parameters. The figure shows that $|\dot{R}|$ appears to blow up at roughly between $R = 0.12$ and 0.13.

6. Discussion

We have considered the Stefan problem for spheres, including the effects of surface tension, motivated in some part by experimental observations concerning the melting of nanoparticles, as reported by Kofman et al. (1999). By setting up experiments based on dark-field electron microscopy, Kofman et al. (1999) found that once the temperature of the particle reached a certain value, the remaining solid core melted abruptly. It may be that our prediction of self-superheating in the solid particles offers a possible explanation for these peculiar observations. It would be interesting to measure the temperature profile inside the solid core of a nanoscaled (spherically-shaped) cluster under melting conditions, with the goal of detecting a superheated temperature profile; at this stage such measurements do not seem possible.

A most interesting result of our study is that the addition of surface tension in the full two-phase Stefan model leads to superheating in the solid phase, and in fact our numerical computations suggest that the solution will cease to exist when the particle radius reaches some critical value R_c (with the corresponding time $t_c < \infty$). This form of finite-time blow-up is well-known to occur in some one-dimensional Stefan problems with superheating. For

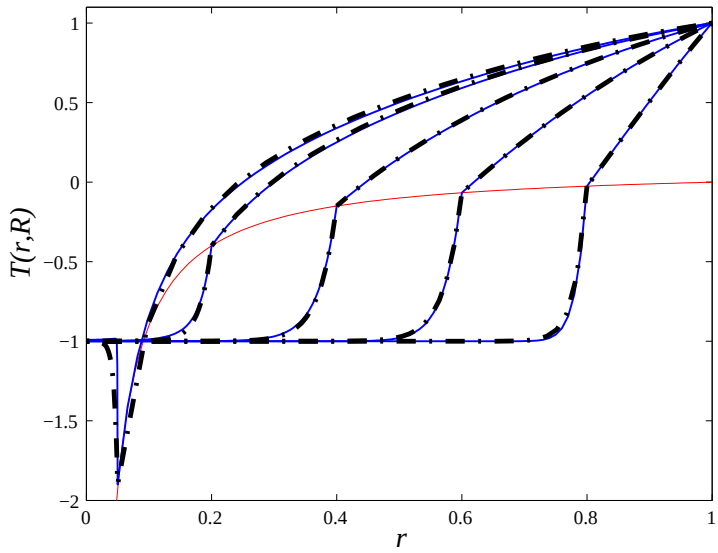

FIG. 4. Temperature profiles for $\alpha = 1$, $\kappa = 0.05$, $\delta = 1$, $V = -1$, $\sigma = 0.1$. The solid curves indicate the numerical solution to the full two-phase problem (2.11)-(2.17), while the dot-dashed curves represent numerical solutions to the limiting the one-phase problem derived in Wu et al. (2008); from right to left, the profiles are for $t = 0.039$, 0.131, 0.237, 0.315 and 0.334. The very thin curve denotes the melting temperature.

example, consider the ill-posed one-phase problem (without surface tension)

$$\frac{\partial T_s}{\partial t} = \frac{\kappa}{\delta}\frac{\partial T_s}{\partial x^2} \quad \text{in} \quad 0 < x < s(t), \tag{6.1}$$

$$T_s = 0, \quad \kappa\frac{\partial T_s}{\partial x} = \alpha\frac{ds}{dt} \quad \text{on} \quad x = s(t), \quad \frac{\partial T_s}{\partial x} = 0 \quad \text{on} \quad x = 0, \tag{6.2}$$

with the initial condition $T_s = V(x) > 0$. It is known (see Fasano & Primicerio 1977, Fasano et al. 1981 and Fasano et al. 1990, for example) that blow-up will occur with $\dot{s} \to -\infty$ as $s \to s_c$, where s_c is some critical size of the domain, if

$$Q = \int_0^1 (V(x) - \alpha)\, dx > 0.$$

In this case there is initially more heat energy in the solid than is required by the solid-melt interface to melt the solid completely. Furthermore, this form of blow-up is still possible for $Q \leqslant 0$ if, for example, the initial condition $V(x)$ has a sufficiently high peak near $x = 1$. Here the situation is that there is a large amount of heat energy concentrated near the interface, and this heat cannot be conducted away fast enough to prevent blow-up. In a similar vein, for our own problem it may be that the melting temperature decays sufficiently quickly that blow-up will always occur, regardless of the initial temperature, as there will come a time when too much heat energy is concentrated near the interface. The exception will be the limiting case

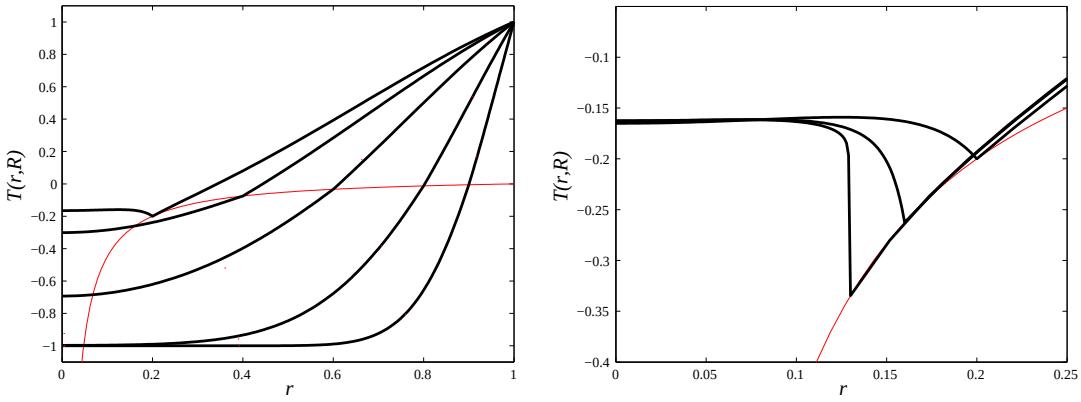

FIG. 5. Temperature profiles for $\alpha = 0.1$, $\kappa = 1$, $\delta = 1$, $V = -1$, $\sigma = 0.05$. The thick curves represent the numerical solution, while the thin curve denotes the melting temperature. Part (a) is drawn for $R = 0.2$ ($t = 0.1306$), 0.4 (0.0114), 0.6 (0.0769), 0.8 (0.0292) and 0.9 (0.0088), while part (b) is for $R = 0.13$ ($t = 0.1314$), 0.16 (0.1312) and 0.2 (0.1306).

$\alpha = \infty$, for which there can never be more heat in the solid than is required to melt it, and presumably blow-up will not occur.

We note that the complete asymptotic structure of (6.1)-(6.2) near blow-up has been documented by Herrero & Velázquez (1996) and King & Evans (2005), for example, with the use of a Baiocchi transform, the result being that

$$s(t) - s_c \sim 2(t_c - t)^{1/2} \ln^{1/2}(-\ln(t_c - t)) \quad \text{as} \quad t \to t_c^-.$$

Notice the length scale that arises does not behave as the square root of time, which is unusual for Stefan problems. The inclusion of surface tension in our model prevents such a Baiocchi transform based approach here, and it is expected that the corresponding analysis for our problem will be more complicated. However, we do anticipate that

$$T_\ell \sim \sigma\left(1 - \frac{1}{r}\right) \quad \text{for} \quad r - R(t) \ll 1 \quad \text{as} \quad t \to t_c^-,$$

leaving a one-phase problem for the temperature in the solid, namely (2.12), (2.14), (2.16), the modified Stefan condition

$$\kappa \frac{\partial T_s}{\partial r} = \frac{dR}{dt}\left(-\frac{\sigma(1-\delta)}{R} + \alpha\right) + \frac{\sigma}{R^2} \quad \text{on} \quad r = R(t),$$

and an appropriate initial condition. We leave these issues to be dealt with elsewhere.

It is worth emphasising that the motivation for including surface tension in some other studies has been to regularise the ill-posed problem of melting a superheated solid (or, equivalently, freezing a supercooled liquid), with the goal of smoothing (unphysical) singularities, or preventing blow-up from occuring. In contrast, the present melting problem (with zero surface tension) is well-posed, and it is in fact the inclusion of surface tension that drives the superheating, and hence is responsible for the solutions to blow up before complete melting can take place. This

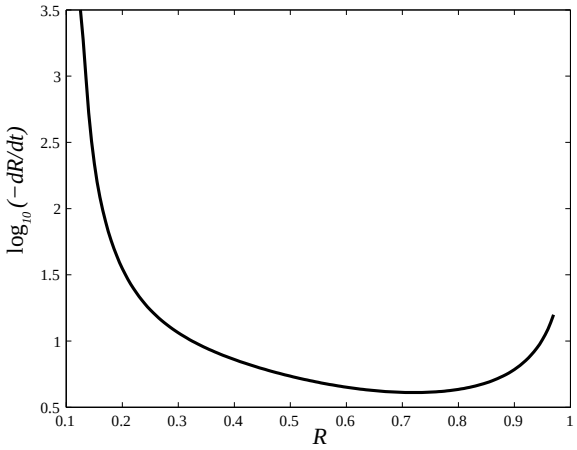

FIG. 6. Plot of the interface speed $\log_{10}(-\dot{R})$ versus R for $\alpha = 0.1$, $\kappa = 1$, $\delta = 1$, $V = -1$, $\sigma = 0.05$.

appears to be a novel feature of the model (at least for Stefan problems). It may be that the addition of some other form of regularisation mechanism (such as kinetic undercooling) in our problem would enable the blow-up to be suppressed, so that the solution could be continued past the blow-up region in the classical sense; however, for real particles the continuum hypothesis would ultimately break down at some stage, so this question is likely to be of more interest to mathematicians than physicists.

A number of points regarding one-phase models are worth repeating. First, when the effects of surface tension are included at the solid-melt interface, there can never be a true one-phase problem, as there will be always be temperature variations in both phases. However, Evans & King (2000) derived a one-phase problem that arises by taking the singular limit of slow conduction in the solid phase ($\kappa \to 0$), and this problem was analysed by the present authors in Wu et al. (2008) for radially symmetric geometries. We have provided in the present paper numerical results that show strong agreement between the one-phase model and the full two-phase model for small values of κ. As mentioned in the Introduction, it is noteworthy that some authors treat the one-phase problem that arises by setting $\kappa = 0$ in (2.15) and ignoring (2.12), however this problem does not conserve heat at the interface. For example, Herraiz et al. (2001) analysed the near-complete-melting limit of that (unphysical) one-phase problem. There is no finite-time blow-up for that problem, and the scalings derived by Herraiz et al. (2001) are not appropriate to either the one-phase problem treated in Wu et al. (2008) or the full two-phase problem studied presently.

Of particular interest would be to generalise the current study to the problem of melting an arbitrary shaped three-dimensional particle. For the classical case with zero surface tension, the one-phase problem has been considered by Andreucci et al. (2001) and McCue et al. (2005) (the two-dimensional analogue is treated in McCue et al. 2003). In that case the solution continues to exist right up to complete melting, and these authors show that in general, the solid-melt interface approaches an ellipsoid in shape in the near-complete-melting limit. However, given the numerical results presented in the present paper, one may expect that the solution for

the more general three-dimensional problem to blow-up in a similar manner, and it may be that the surface tension drives the melting process to be radially symmetric just before blow-up, regardless of the initial geometry. On the other hand, it may be that self-superheating in the more general three-dimensional problem is responsible for the onset of a cusp, perhaps accompanied by another form of blow-up. These questions remain unanswered, and are left for future research.

Acknowledgements

BW and JMH acknowledge the support from the Discovery Project scheme of the Australian Research Council and JMH is grateful for the provision of an Australian Professorial Fellowship. The authors thank Dr Pei Tillman for reading through an earlier version of the manuscript, and for her fruitful suggestions.

References

Andreucci, D., Herrero, M. A. and Velázquez, J. J. L. (2001) The classical one-phase Stefan problem: a catalog of interface behaviors. *Surv. Math. Ind.*, **9**, 247-337.

Buffat, P.A & Borel, J.P. (1976) Size effect on the melting temperature of gold particles. *Phys. Rev. A.* **13**, 2287-2298.

Carslaw, H.S. & Jaeger, J.C. (1959) Conduction of heat in solids. *Oxford:Clarendon Press.*

Crank, J. (1984) Free and moving boundary problems. *Oxford:Clarendon Press.*

Davis, G.B. & Hill, J.M. (1982) A moving boundary problem for the sphere. *IMA J. Appl. Math*, **29**, 99-111.

Dewynne, J.N. (1985) On an integral formulation for heat-diffusion moving boundary problems. *Ph.D thesis*, University of Wollongong, NSW, Australia.

Dewynne, J.N., Howison, S.D., Ockendon, J.R. & Xie, W. (1989) Asymptotic behaviour of the solutions to the Stefan problem with a kinetic condition at the free boundary. *J. Aust. Math. Soc.* B, **31**, 81-96.

Dippel, M., Maier, A., Gimple, V., Wider, H., Evenson, W.E., Rasera, R.L. & Schatz, G. (2001) Size-dependent melting of self-assembled indium nanostructures. *Phys. Rev. Lett.*. **87**, 095505.

Evans, J.D. & King, J.R. (2000) Asymptotic results for the Stefan problem with kinetic undercooling. *Q. J. Mech. Appl. Math.*. **53**, 449-473.

Fasano, A. & Primicerio, M. (1977) General free boundary problems for the heat equation. I. *J. Math. Anal. Appl.*, **57**, 694-723.

Fasano, A., Primicerio, M. & Lacey, A.A. (1981) New results on some classical parabolic free boundary problems. *Q. Appl. Math.*, **38**, 439-460.

Fasano, A., Primicerio, M., Howison, S.D. & Ockendon, J.R. (1990) Some remarks on the regularization of supercooled one-phase Stefan problems in one dimension. *Q. Appl. Math.*, **48**, 153-168.

Gupta, S.C. (2003) The Classical Stefan Problem: Basic Concepts, Modelling and Analysis. Amsterdam: Elsevier.

Herraiz, L.A., Herrero M.A. & Velázquez, J.J.L. (2001) A note on the dissolution of spherical crystals. *Proc. Roy. Soc. Edin.* **131** 371-389.

Herrero, M.A. & Velázquez, J.J.L. (1996) Singularity formation in the one-dimensional supercooled Stefan problem. *Euro. J. Appl. Math.*, **7**, 119-150.

Herrero, M.A. & Velázquez, J.J.L. (1997) On the melting of ice balls. *SIAM J. Math. Anal.*, **28**,

1-32.

Herrero, M.A., Medina, E. & Velázquez, J.J.L. (2000) The birth of a cusp in the two-dimensional, undercooled Stefan problem. *Q. Appl. Math.*, **58**, 473-494.

Howison, S.D., Ockendon, J.R. & Lacey A.A. (1985) Singularity development in moving boundary problems. *Q. J. Mech. Appl. Math.*, **38**, 343-360.

King, J.R. & Evans, J.D. (2005) Regularization by kinetic undercooling of blow-up in the ill-posed Stefan problem. *SIAM J. Appl. Math.*, **65**, 1677-1707.

Kofman, R., Lereah, Y., Stella, A. (1999) Melting of clusters approaching 0D. *Eur. Phys. J. D.* **9**, 441-444.

Kucera, A. & Hill, J.M. (1986) On inward solidifying cylinders and spheres initially not at their fusion temperature. *Int. J. Non-linear Mech.*, **21**, 73-82.

Langer, J.S. (1950) Instabilities and pattern formation in crystal growth. *Rev. Mod. Phys.*, **8**, 81-94.

McCue, S.W., King, J.R. & Riley, D.S. (2003) Extinction behaviour for two-dimensional solidification problems, *Proc. R. Soc. Lond.* A, **459**, 977-999.

McCue, S.W., King, J.R. & Riley, D.S. (2005) The extinction problem for three-dimensional inward solidification. *J. Eng. Math.*, **52**, 389-409.

McCue, S.W., Wu, B. & Hill, J.M. (2008) Classical two-phase Stefan problem for spheres. *Proc. R. Soc. Lond.* A, **464**, 2055-2076.

Meyer, G.H. (1973) Multidimensional Stefan problems. *SIAM J. Numer. Anal.*, **10**, 522-538.

Nanda, K.K., Sahu, S.N. & Behera, S.N. (2002) Liquid-drop model for the size-dependent melting of low-dimensional systems. *Phys. Rev. E*, **66**, 013208.

Olson, E.A., Efremov, M.Y., Zhang, M., Zhang, Z. & Allen, L.H. (2005) Size-dependent melting of Bi nanoparticles. *J. Appl. Physi.* **97**, 034304.

Riley, D.S., Smith, F.T. & Poots, G. (1974) The inward solidification of spheres and circular cylinders. *Int. J. Heat Mass Transfer*, **17**, 1507-1516.

Smith, G.D. (1985) Numerical Solution of Partial Differential Equations: Finite Difference Methods. Oxford: Clarendon Press.

Soward, A.M. (1980) A united approach to Stefan's problem for spheres and cylinders. *Proc. R. Soc. Lond.* A, **373**, 131-147.

Stewartson, K. & Waechter, R.T. (1976) On Stefan's problem for spheres. *Proc. R. Soc. Lond.* A, **348**, 415-426.

Velázquez, J.J.L. (1997) Cusp formation for the undercooled Stefan problem in two and three dimensions. *Euro. J. Appl. Math.* **8**, 1-21.

Voller, V. & Cross, M. (1981) Accurate solutions of moving boundary problems using the enthalpy method. *Int. J. Heat Mass Transfer.* **24**, 545-556.

Wronski, C.R.M. (1967) The size dependence of the melting point of small particles of tin. *Br. J. Appl. Phys.* **18**, 1731-1737.

Wautelet, M. (1991) Estimatiion of the variation of the melting temperature with the size of small particles, on the basis of a surface-phonon instability model. *J. Phys. D.* **24**, 343-346.

Wu, B., McCue, S.W., Tillman, P. & Hill, J.M. (2008) Single phase limit for melting nanoparticles. *Appl. Math. Mod.*, doi:10.1016/j.apm.2008.07.009.

Wu, T., Liaw, H.C. & Chen, Y.Z. (2002) Thermal effect of surface tension on the inward solidification of spheres. *Int. J. Heat Mass Transfer.* **45**, 2055-2065.

Zhang, M., Efremov, M.Y., Schiettekatte, F., Olson, E.A., Kwan, A.T., Lai, S.L., Wisleder, T., Greene, J.E., Allen, L.H. (2000) Size-dependent melting point depression of nanostructures: Nanocalorimetric measurements. *Phys. Rev. B.* **62**, 10548-10557.